Published in final edited form as:
Invest Ophthalmol Vis Sci. 2008 April ; 49(4): 1686–1695. doi:10.1167/iovs.07-1058.

Elevated MMP Expression in the MRL Mouse Retina Creates a Permissive Environment for Retinal Regeneration

Budd Tucker[1], **Henry Klassen**[2], **Liu Yang**[1,3], **Dong Feng Chen**[1], and **Michael J. Young**[1]

1*Department of Ophthalmology, Schepens Eye Research Institute, Harvard Medical School, Boston, Massachusetts*

2*Department of Ophthalmology, School of Medicine, University of California, Irvine, California*

3*Department of Ophthalmology, Peking University First Hospital, Beijing, People's Republic of China*

Abstract

Purpose—The MRL/MpJ (healer) mouse is an established model for autoimmune studies and was recently identified as having a profound ability to undergo scarless regeneration of the tissue in the ear and heart. This regenerative capacity has been linked to elevated matrix metalloproteinase (MMP)-2 and -9 expression, giving this mouse the ability to degrade and remove inhibitory basement membrane molecules. Although elevated MMP expression has been reported in somatic tissues in this strain, little is known about MMP expression and the response to injury in the MRL/MpJ mouse retina. The purpose of this study was to investigate whether increased MMP expression and subsequent decreased inhibitory extracellular matrix molecule deposition in the MRL/MpJ mouse retina produces a permissive regenerative environment.

Methods—Experiments were performed using 3- to 4-week-old MRL/MpJ, retinal degenerative (rd1), and C57BL/6 (wild-type) mice. Western blotting, oligo-microarray, and immunohistochemical analyses were used to determine the level and location of MMP and extracellular matrix (ECM) protein expression. Retinal responses to injury were modeled by retinal detachment in vivo and in retinal explantation in vitro. The capacity of the retinal environment to support photoreceptor cell migration, integration, or regeneration was analyzed using hematoxylin-eosin, immunohistochemical staining, and cell counting.

Results—Compared with C57BL/6J animals, MRL/MpJ mice exhibit elevated levels of MMP-2, -9, and -14 and decreased levels of the inhibitory proteins neurocan and CD44 within the retina. Although similar increases in MMP-2, -9, and CD44s (CD44 degradation product) were observed in the rd1 retina, elevated levels of the inhibitory ECM molecules (neurocan and CD44) remained. Thus, the MRL retinal environment, which expresses lower levels of inhibitory ECM molecules after injury, was more conducive to regeneration and enhanced photoreceptor integration in vitro than C57BL/6J or rd1 controls.

Conclusions—The MRL mouse retina shows elevated MMP expression and decreased levels of scar-related inhibitory molecules, which leads to a retinal environment that is more permissive for neural regeneration and cell integration after in vitro retinal explantation.

Correspondence to: Michael J. Young.

Corresponding author: Michael J. Young, Department of Ophthalmology, Schepens Eye Research Institute, Harvard Medical School, 20 Staniford Street, Boston, MA 02114; michael.young@schepens.harvard.edu..

Disclosure: **B. Tucker**, None; **H. Klassen**, None; **L. Yang**, None; **D.F. Chen**, None; **M.J. Young**, None

The publication costs of this article were defrayed in part by page charge payment. This article must therefore be marked "*advertisement*" in accordance with 18 U.S.C. §1734 solely to indicate this fact.

It is well known that the regenerative capacity of the adult mammalian central nervous system (CNS) is extremely restricted and generally limited to aberrant local sprouting. This inability to regenerate can be attributed to an assortment of factors, including enhanced expression of inhibitory extracellular matrix (ECM) and cell adhesion molecules, many of which are injury-induced factors found in areas of glial hypertrophy and scar formation. Of the injury-induced inhibitory molecules, the chondroitin sulfate proteoglycans (CSPGs) such as neurocan and the hyaluronan-binding glycoprotein CD44 are particularly abundant.[1,2] These molecules have previously been shown to function as chemical inhibitors of neurite and axonal growth, preventing functional regeneration of a number of different cell types.[1,3] Moreover, inhibition of these molecules, or their hyaluronan-expressing targets, has been shown to enhance axonal regeneration in a variety of instances, thereby alleviating molecularly induced growth inhibition.[2,4]

Like the brain and spinal cord, the retina is part of the central nervous system and also produces these growth inhibitory molecules. Both neurocan and CD44 are expressed in the normal retina and there, as in other CNS locations, injury stimulates the increased production of these proteins by reactive glial cells, in this case retinal astrocytes and radial Müller glia.[5-11] For example, the C3H/HeJ (retinal degenerative [rd1]) mouse, which undergoes rapid degeneration of the photoreceptor layer, is known to experience glial scar formation and enhanced expression of CD44 and neurocan at the far periphery of the remaining retina.[6,7,11,12] Upregulation of these inhibitory molecules creates an inhospitable environment for growing neurites, hindering successful retinal transplantation by largely blocking donor-host integration.[12] Thus, to induce regeneration and restore visual function through transplantation, neutralization of these inhibitory proteins is necessary.

A family of proteins well known for their ability to degrade ECM and cell adhesion molecules are the zinc-dependent matrix metalloproteinases (MMPs). As many as 24 different MMPs, subclassified into at least five distinct groups (gelatinases, stromelysins, collagenases, membrane-type, “other”) have been identified.[13,14] Of the substrates targeted by MMPs, the inhibitory CSPGs and CD44 are included.[15-19] For instance, the membrane-bound MMP-14 has previously been shown to induce CD44 shedding in vitro, thus stimulating enhanced tumor cell migration.[17,18] Both MMP-2 and MMP-9 have been shown to degrade CSPGs such as neurocan, unmasking their inhibitory effect on laminin-induced neurite outgrowth from peripheral sensory neurons.[15] Similarly, in a series of in vivo experiments, we have previously shown that stem cell-induced MMP-2 production results in CD44 and neurocan degradation, removing the inhibitory ECM molecule barrier deposited at the level of the outer limiting membrane of the degenerating retina and stimulating integration between host and transplanted tissue.[12]

More extreme examples of MMP-induced regeneration can be found in many lower vertebrates such as salamanders and newts, which have the ability to regenerate entire limbs after amputation.[20-24] Although this striking ability to achieve complete regeneration is normally limited to more primitive organisms, a mammalian model of body tissue regeneration and wound repair has been identified. The MRL/MpJ (MRL; healer) mouse, an established model for autoimmune studies, has recently been shown to undergo scarless regeneration and tissue replacement of the ear and heart.[25-30] In the case of normal C57BL/6J (BL6) mice, the tissue defects created by 2-mm through-and-through ear punches, as are used for identification, typically remain patent throughout the life of the animal and are demarcated by scar formation at the margin of the injured tissue.[25] In the healer mouse, however, this is not the case. Thirty days after injury, complete scarless regeneration is seen, characterized by normal-appearing ECM deposition, vascular reconstruction, and cartilage growth.[25] As in lower vertebrates, this phenomenon has been linked to elevated MMP levels, predominantly MMP-2 and -9, which are responsible for ECM remodeling and removal of inhibitory basement membrane molecules.

Although this is the case for skin and heart, little is known about the level of expression and involvement of MMPs in the retina of the MRL mouse. Therefore, we hypothesize that the elevated MMP expression observed in other body tissues would also be present in the MRL retina and that subsequently there would be decreased levels of inhibitory basement membrane molecules such as CD44 and neurocan, resulting in a more conducive environment for transplantation and neuronal regeneration after retinal injury.

Materials and Methods

Animals

MRL mice, 3 to 4 weeks of age, were used as experimental animals, and age-matched retinal degenerative C3H/HeJ (rd1) and BL6 mice (Jackson Laboratory, Bar Harbor, ME), were used as injury and wild-type controls, respectively. GFP-positive BL6 mice (GFP-positive) were used as photoreceptor sheet donors (original breeders were purchased from the Jackson Laboratory; all experimental donors were collected from the subsequent in-house breeding colony). To complete the studies 48 MRL, 42 rd1, 48 BL6, and 6 GFP-positive mice were used. All experiments were conducted with the approval of the Schepens Eye Research Institute Animal Care and Use Committee and the ARVO Statement for the Use of Animals in Ophthalmic and Vision Research.

Photoreceptor Sheet Explant Isolation

Photoreceptor sheets were isolated from adult GFP-positive mice using procedures described elsewhere ($n = 6$).[31,32] Briefly, retinas from 30- to 60-day-old GFP-positive mice were carefully dissected and flattened by making four radial cuts. Flattened retinas were placed, photoreceptor side down, on a 20% gelatin block that had previously been secured to a vibratome chuck. A 4% gelatin solution was flushed under the retina with a flame-polished Pasteur pipette and aspirated immediately. The gelatin was allowed to dry for at least 2 minutes to allow the retina to adhere to the underlying base, and the vibratome bath was subsequently filled with ice-cold CO_2 independent media (Invitrogen). The vibratome chamber was kept at 4°C to prevent the gelatin from melting and the retina from detaching. Starting at the vitreal surface, sequential 20- to 50-μm sections were cut until the photoreceptor layer was reached (approximately 120 μm in depth; the appropriate retinal layer was determined by microscopic analysis of each section and remaining tissue). When the photoreceptor layer was reached, a 200-μm-thick section was taken, and the photoreceptor layer and attached gelatin sheet was collected. Isolated photoreceptor sheets were then used for abutting retinal explant experiments.

Explant Cultures

The procedure used for retina explant cultures has been described previously.[33,34] Briefly, retinas from adult, BL6 ($n = 42$ animals), rd1 ($n = 42$ animals), and MRL ($n = 42$ animals) mice were dissected free from donor eyes, transferred to freshly prepared serum-free modified neurobasal media, and cut into four equal-sized pieces. Each piece of retina was mounted onto tissue culture plate inserts (Millicell-CM Organotypic; Millipore, Billerica, MA) with the vitreal surface of the explant closest to the filter. Cultures were plated in the absence or presence of GFP-positive photoreceptor sheets, which were placed on the outer (subretinal) surface of the retina and incubated in serum-free modified neurobasal medium at 37°C with 5% CO_2 for 7 days. Depending on the experimental condition, cultures were subsequently processed for Western blot or immunohistochemical analysis.

Retinal Detachments

This procedure was the only in vivo analysis performed in these studies and was performed as described previously.[35] Briefly, BL6 and MRL mice were anesthetized by intraperitoneal injection of a mixture of ketamine (62.5 mg/kg; Webster Veterinary Supply, Sterling, MA) and xylazine (12.5 mg/kg; Webster). Right eyes were anesthetized and pupils were dilated with topical application of 0.5% proparacaine (Akorn, Buffalo Grove, IL) and 1% tropicamide (Akorn), respectively. A scleral perforation was created in the superior-temporal quadrant to lower intraocular pressure. A glass micropipette was then advanced into the vitreous through the retina and into the subretinal space under microscopic visualization, where 1 to 2 μL of 1.4% sodium hyaluronate (Healon GV; Pharmacia & Upjohn, Uppsala, Sweden; a viscous material used during intraocular surgery in humans and not associated with any known ocular toxicity) was injected between the retina and the retinal pigment epithelium (RPE). After surgery, mice were placed in clean cages and allowed to recover in a prewarmed environment before they were returned to their original housing room. The experiment was terminated at 14 days after surgery, eyes were enucleated, and immunohistochemical analysis was performed (n = 6 animals per group; further description of these animals is included in the immunohistochemical analysis section).

Immunohistochemistry

Tissue fixation, sectioning, and immunocytochemistry were performed on whole eyes (n = 6 BL6 animals and 6 MRL animals, postretinal detachment) and retinal explants (n = 6 BL6 animals, 6 rd1 animals, and 6 MRL animals). Tissue was fixed in 4% paraformaldehyde in PBS and cryoprotected in sequential 10% and 25% sucrose solutions. Tissue was embedded, cryosectioned, and immunostained as described previously[36] with CD44 (1:100; BD PharMingen, San Diego, CA) and neurocan (1:100; gift from Richard Margolis, Department of Pharmacology, New York University). Sections were subsequently incubated in either Cy3- or Cy5-conjugated secondary antibodies (1:100; Jackson ImmunoResearch, West Grove, PA) and were analyzed using confocal microscopy. To control for experimenter bias, microscopic analysis was performed in such a way that exposure time, gain, and depth of field remained constant between experimental conditions. Similarly, for each experiment, all staining was performed at the same time using the same staining parameters. When compiling each figure with the use of graphics software (Adobe Photoshop; Adobe Corp., Mountain View, CA), all data were processed in the same way.

Cell Counting

Cell counts (see Fig. 5) were performed by counting the total number of cells that crossed the host donor border in 12 randomly selected microscopic fields taken from each experimental repeat. Therefore, the analysis was based on 36 microscopic fields for each experimental condition.

Immunoblotting

For Western blot analyses, retinas from retinal explants were homogenized in lysis buffer (50 mM Tris-HCl, pH 7.6, 150 mM NaCl, 10 mM CaCl2, 1% Triton X-100, 0.02% NaN_3) and centrifuged, supernatants were isolated, and protein concentrations were determined using a BCA protein assay (Pierce Chemical, Rockford, IL; n = 24 BL6 animals, 24 rd1 animals, and 24 MRL animals). Equivalent amounts of protein (50 μg) were subjected to SDS-PAGE (8%-10% acrylamide), transferred to nitrocellulose, and probed with the following antibodies: CD44S (1:1000; Sigma), neurocan (1:1000; gift from Richard Margolis, Department of Pharmacology, New York University), pro-MMP-2, pro-MMP-9, pro-MMP-14 (1:1000; Chemicon), and β-actin (1:1000, used as a loading control; Abcam, Cambridge, MA). Blots were cut and reprobed sequentially, visualized with ECL reagents (NEN, Boston, MA), and

exposed to x-ray film (Kodak/Carestream Health, Bio Max Light Film, Rochester, NY). Developed films were subsequently digitized and densitometrically analyzed with Image J software (National Institutes of Health; each substrate was normalized against β-actin). Digital images of Western blots were used to make composite figures with graphics software (Adobe Photoshop; Adobe Corp.).

ECM Array Screening for Gene Expression

Biotin-tagged cRNA, synthesized from total RNA collected from BL6 (n = 12 animals), rd1 (n = 12 animals), and MRL (n = 12 animals) mouse retinal explants, was bound to ECM oligo-arrays by hybridization at 60°C for 12 to 16 hours (SuperArray Bioscience, Frederick, MD) and subsequently imaged using chemiluminescence and x-ray film detection (Kodak). Films were digitized and uploaded to Web-based analysis software (SuperArray Bioscience), and densitometric data were subsequently analyzed using one-way ANOVA with Tukey testing for post hoc comparisons. To control for experimental variation (e.g., exposure/CRNA loading), densitometric analyses for each probe were corrected against internal housekeeping genes located on each microarray.

Statistical Analysis

Each experiment, with the exception of those reported (see Fig. 4), was repeated three times using a minimum of four retinas per experimental condition. Figure 4 shows data on six animals per experimental group; unlike the other experiments in this study, the procedures depicted here were performed in vivo. Only one eye per animal could be used during surgery, resulting in a total of six eyes per experimental condition. Contralateral nonsurgery eyes were used as noninjury controls. Where appropriate, data are plotted as mean ± SEM and significance is noted only if $P \leq 0.05$, as determined by one-way ANOVA with Tukey testing for post hoc comparisons (n = number of retinas used in each experimental condition).

Results

Elevated MMP-2, MMP-9, and MMP-14 Expression in the MRL Mouse Retina

A mass screen of all known MMPs was performed using a focused oligo microarray system (SuperArray Bioscience) to examine whether MMP expression was elevated in the MRL mouse retina compared with rd1 mice and BL6 controls. As has been suggested,[12,13,17,18] MMP-2, -9, and -14 together have the ability to digest the inhibitory CSPGs, neurocan, and the glycoprotein CD44. For this reason, we have chosen to focus on these molecules. As a further control, we have also chosen to include MMP-13, which shows a pattern of expression contrary to that of the MMPs mentioned. As shown in Figure 1A-E, significant differences in the levels of MMP mRNA expression were identified. For instance, retinal expression of MMP-2 (Figs. 1A, 1B), MMP-9 (Figs. 1A, 1C), and MMP-14 (Figs. 1A, 1D) RNA were all significantly higher in MRL and rd1 mice than in BL6 controls. MMP-13 mRNA (Figs. 1A, 1E), however, was significantly lower in MRL and rd1 mice than in BL6 controls.

Western blot analysis of MRL, rd1, and BL6 retinal tissue was carried out using 7-day retinal explant cultures to determine whether similar results were observed at the level of MMP enzyme expression. As seen in the previous microarray analysis, MMP-2 (Fig. 2A) and MMP-9 (Fig. 2B) expression was significantly higher in MRL and rd1 mouse retina than in BL6 wild-type controls. However, unlike the result obtained from mRNA analysis, the level of MMP-14 (Fig. 2C) expression was significantly higher in the MRL mouse retina only, and there was no significant difference in retinal MMP-14 expression between rd1 and BL6 animals. Collectively, these results indicate that elevated MMP expression was found in the MRL retina, as indicated by freshly isolated and 7-day post-explant tissue.

Decreased Expression of the Inhibitory ECM Molecules CD44 and Neurocan in the MRL Mouse Retina

To determine whether elevated MMP expression in the MRL mouse retina led to increased degradation of inhibitory ECM molecules, including CD44 and neurocan, a series of in vitro experiments using Western blotting and immunohistochemistry of retinal explants was performed. As indicated in Figure 3A-C, a significant increase in CD44s (Fig. 3A), the degradation product of CD44, was seen in MRL and rd1 retinas compared with BL6 controls. Elevated neurocan-CT (Fig. 3B), the degradation product of neurocan, and decreased full-length neurocan (Fig. 3C) were also detected in the retinas of MRL mice compared with BL6 and rd1 animals. Interestingly, no significant change in neurocan degradation or increased full-length neurocan expression was detected in rd1 compared with BL6 controls, even though MMP elevation was observed.

Similar results were observed with evaluations of full-length CD44 and neurocan expression immunohistochemically (Figs. 3D-I). In accordance with increased CD44 and neurocan degradation, decreased expression of these proteins was detected in MRL (Figs. 3F, 3I) retinas compared with BL6 (Figs. 3D, 3G) and rd1 (Figs. 3E, 3H) controls. Most notable is the decrease in expression at the outer nuclear/photoreceptor layers; only a thin band of CD44 staining remains at the base of the MRL photoreceptor layer (Fig. 3F, arrowheads), with very faint staining seen at the level of the outer segments (Fig. 3F, arrows). This is in contrast to the much denser expression of this protein in rd1 and BL6 controls (Fig. 3D, arrows and arrowheads). It is important to note that although elevated levels of CD44s were detected in rd1 retinas, substantially more CD44 expression was still detected in these animals than in their BL6 counterparts, especially at the outer nuclear layer of the degenerated retina (Fig. 3E, arrows). Similarly, neurocan staining was more intense and was expressed throughout the entire retina. These data suggest that MRL retinas may present an environment that would be less inhibitory to regeneration than those of wild-type and rd1 mice after injury.

Retinal Detachment-Induced Formation of a Hypertrophic Glial Barrier Is Inhibited in the MRL Mouse Retina

To study whether elevated MMP expression in the MRL mouse retina acts to degrade neurocan and CD44 in vivo and, in parallel, inhibit glial hypertrophy, we selected a model of retinal detachment. As seen after a variety of insults throughout the CNS, experimental retinal detachment stimulates glial cell reactivity, which coincides with injury-induced deposition of the CSPG neurocan and upregulation of CD44.[10,37,38] Here, a series of retinal detachment experiments were performed to evaluate this same phenomenon in the context of the murine retina. Compared with uninjured controls (Fig. 4A), an increase in CD44 (red) and neurocan (blue) staining was detected in BL6 animals after retinal injury, including both the injection site (Fig. 4C) and area immediately adjacent, where the retinal detachment was created (Fig. 4E). CD44 staining was most intense at glial cell outer limits, both at the injection site (Fig. 4C, arrowheads) and immediately adjacent in areas of detachment (Fig. 4E, arrowheads). Intense neurocan deposition, encompassing the outer limits of the photoreceptor layer, was also identified (Figs. 4C, 4E, arrows). Unlike BL6 counterparts, when compared with controls (Fig. 4B) no significant increase in CD44 or neurocan expression were detected in MRL mice after retinal injury (Figs. 4D, 4F). For instance, the intense band of CD44 staining found adjacent to the outer limiting membrane of BL6 animals after injury (Figs. 4C, 4E, arrowheads) was less prominent and almost completely abolished in MRL mice at both injection (Fig. 4D, arrowheads) and detachment (Fig. 4F, arrowheads) sites. Similarly, neurocan staining, which was detected in the outer retinas of injured BL6 animals (Figs. 4C, 4E, arrows), was less intense and almost absent in injured MRL mice (Figs. 4D, 4F, arrows).

Interestingly, the intensity of neurocan staining in vascular tissue (retinal vasculature staining with neurocan was previously shown in RCS rats[9]) was identical in BL6 (Figs. 4C, 4D, arrowheads with asterisks) and MRL (Figs. 4E, 4F, arrowheads with asterisks) animals after injury. Thus, elevated MMP expression in the MRL retina is associated with significantly less inhibitory ECM deposition and reduced formation of a hypertrophic glial barrier at the level of the outer limiting membrane than in BL6 animals after injury in vivo.

Enhanced Photoreceptor Cell Migration in the MRL Mouse Retina Compared with rd1 and BL6 Controls

Next, we asked whether the MRL retina presents a less inhibitory or more conducive environment for neuronal regeneration and migration than BL6 and rd1 retinas. As a first step, we took a traditional approach that evaluated retinal regenerative capacity in explant cultures.

A series of abutting retinal explant experiments was performed in which GFP-positive photoreceptor sheets were placed on top of B6, rd1, or MRL mouse retinas. These cultures were incubated in serum-free neurobasal media for 7 days and subsequently analyzed for cellular migration and integration by confocal microscopy and cell counting. A significant increase in the number of adult GFP-positive photoreceptor cells migrating into the MRL (Figs. 5C, 5D) compared with BL6 (Figs. 5A, 5D) and rd1 (Figs. 5B, 5D) mouse retinas was observed. For instance, unlike abutting BL6 (Fig. 5A) and rd1 (Fig. 5B) explant cultures, which showed little to no photoreceptor cell integration, abutting MRL (Fig. 5C) cultures showed extensive incorporation, with cells migrating up to 110 μm beyond the MRL-photoreceptor transplant margin (as measured from the dotted line to the innermost cell marked with an arrow in Fig. 5C). These findings suggest that elevated MMP expression and subsequent decreased inhibitory ECM molecule deposition is conducive to the integration of transplanted photoreceptor sheets, a phenomenon seen in the mature MRL retina but not in controls. Interestingly, though elevated MMP expression was detected in the rd1 mouse retina (Fig 2) elevated levels of inhibitory ECM molecules persisted, preventing host transplant integration.

Discussion

The ability of the MRL mouse to undergo complete scarless regeneration of the ear after a 2-mm through-and-through ear punch was initially identified by Clark and colleagues[25-27] as resulting from elevated MMP expression (predominantly types 2 and 9) and subsequent ECM remodeling.[25-27] Although we show that retinal injuries do not heal to the same degree, a variety of MMP and ECM differences have been identified. To summarize our results, a diagram depicting our findings has been included. As shown in Figure 6, enhanced MMP-2, -9, and -14 (MMP-14, which was not previously identified in this model) expression was identified within the retina of the MRL mouse, which inhibited injury-induced glial hypertrophy and resulted in increased degradation and decreased expression of the inhibitory ECM molecules CD44 and neurocan.

It is important to note that although elevated MMP-2 and -9 were also seen in rd1 animals after retinal explant experiments, significant elevations of CD44 and neurocan were still observed in these retinas (as shown in Figs. 3D, 3E). This is potentially because, unlike the MRL, there was no significant elevation of MMP-14 (Fig. 2C). Aside from its ability to degrade ECM molecules itself, MMP-14 is known to cleave and subsequently activate various MMPs, especially MMP-2.[39] Thus, decreased levels of this molecule may result in a paucity of active MMPs at the injury site, accounting for the lack of inhibitory ECM removal in this animal. If this were the case, one could envision how endogenously elevated MMP-2 and -9 in the rd1 animal could be targeted to stimulate inhibitory ECM removal, thus creating a more permissive regenerative environment. For instance, activation of these enzymes can be achieved by exogenous delivery of a variety of different molecules, including the plasminogen activators

tPA and uPA, which are often used in patients who have had strokes.[40,41] These molecules have been shown to activate MMP-2 and -9 both directly, through pro-domain cleavage, and indirectly, through MMP-14 induction. Thus, by directly delivering these agents to the degenerative rd1 retina, one could potentially activate endogenously elevated MMP levels, leading to enhanced degradation of CD44 and neurocan and, in turn, creating a postinjury retinal environment that more closely resembles that of the MRL mouse.

However, another plausible reason for elevated CD44 and neurocan expression levels, in spite of increased MMP-2 and -9 levels in the rd1 mouse, is that the rate of ECM production far outweighs the rate of ECM degradation. For instance, it is possible that the rapid, continuous degeneration of the outer retina that occurs in the rd1 mouse is so intense that more of the inhibitory ECM molecules are being deposited than can be processed by the elevated MMP expression. If this is the case, delivery of preactivated ECM-degrading enzymes, such as MMP-2 and -9, may be more beneficial than delivery of the activators of these proteins.

Taken together, these conditions create a retinal environment in the MRL mouse that is more conducive to regeneration than either BL6 or rd1, such as through photoreceptor explantation. Removal of the inhibitory barrier between host and donor tissue allows cellular integration that is not otherwise seen after the donation of mature mammal retina. Evidence for this comes from a series of experiments performed by Aramant et al. [42] that show the capacity of retinal transplants to integrate with host tissue is highly dependent on donor age. For instance, successful graft integration was maximal if donor tissue was isolated at embryonic day 15, diminished after postnatal days 2 to 4, minimal at postnatal day 14, and completely unsuccessful by postnatal day 21.[42] A number of similar studies have since shown that host donor transplant integration can be successful if the donor tissue is taken from various times in embryonic development.[43-49] Although these findings are of interest, a variety of reasons, including ethics and tissue quantity, can explain why we chose to use adult rather than embryonic donor tissue.

Although the present findings support our previous observation that MMP production has the ability to stimulate regeneration through ECM molecule barrier removal and host-donor integration,[12] it should be noted that MMP elevation is not always a positive regenerative event, especially in delicate CNS tissues. For example, it has been shown that the upregulation of MMP-9 after traumatic brain injury is associated with a poorer prognosis, whereas MMP inhibition by chemical inhibitors or gene deletion has the ability to prevent MMP-induced adverse effects.[50,51] Similarly, after focal ischemia, MMP-2 and -9 are rapidly upregulated and associated with increased stroke severity, whereas MMP inhibition has been shown to decrease infarct size and to promote blood-brain barrier integrity after reperfusion.[52-55] Within the retina, similar disruptive MMP effects have also been identified. For example, Fini et al.[56] have shown that increased MMP-9 production by optic nerve ligation stimulates increased retinal ganglion cell death because of the disruption of the supporting laminar structure. This is not the case in MMP-9-deficient mice, which show little to no retinal ganglion cell impairment and more closely resemble normal uninjured animals.[56] Why, then, is elevated MMP expression in the MRL mouse retina not causing retinal disorganization in this animal? It is likely that enhanced MMP expression is under tight regulation by endogenous tissue inhibitors of metalloproteinases (TIMPs). As suggested by Heber-Katz et al.,[57] MMP elevation after ear punch is accompanied by decreased TIMP expression and subsequent enzymatic inhibition. We have observed that in the normal retina before injury, in addition to MMP-2, -9, and -14, TIMP mRNA was highly expressed (data not shown). Although we have not undertaken a complete time course experiment in this animal before and after injury, together these data suggest that, in addition to the basal elevation of MMP mRNA, elevated TIMP expression may help keep the normal retinal architecture intact. We suggest that after injury, decreased TIMP expression releases inhibition of MMP activity, allowing degradation of the

newly expressed inhibitory ECM molecules. After ECM degradation, one would expect that TIMP expression would again rise, preventing further destruction of the remaining retina. Given that we have thus far focused on the effects of MMP elevation on glial scar removal and host-transplant integration, further experimentation is required to confirm this theory.

Although this is the first study to focus on MMP-induced glial barrier removal in the MRL mouse retina, similar studies in other CNS locations have been reported. In a publication by Hampton et al.,[58] cellular changes within the cerebral cortex and striatum after a stab injury were evaluated. It was reported that MRL mice express elevated MMP-2 and -9 mRNA levels adjacent to the injury site compared with controls.[58] Although increased cellular proliferation was found, as indicated by BrdU uptake, there was no significant difference in cortical injury closure, axonal regeneration, or glial scar formation.[58] The different findings with relation to glial responses between the Hampton et al.[58] and the present study could relate to a number of factors, most importantly different compartments of CNS, the specific injury model evaluated, and the definition of glial scar. In any case, the similar findings with regard to MMP expression after retinal injury support our central observations.

Another study of interest, performed by Baker et al.,[59] focused on differences in the CNS in MRL and healthy animals. They evaluated cellular proliferation within the subventricular zone and subsequent migration along the rostral migratory stream. In the MRL mouse, there was enhanced subventricular zone cell proliferation with little to no cell death, resulting in the formation of cellular nests that protruded into the lateral ventricles. To ensure that these protrusions were not caused by migration defects, a series of elegant experiments was performed that looked at cellular entry into, and migration along, the rostral migratory stream. They were able to show abundant incorporation of newly generated neuroblasts into migratory chains, which coincided with significantly enhanced migratory stream diameter and cell number, suggesting that there is actually enhanced cellular migration in the MRL compared with controls. Although this group did not look at differences in cellular MMP expression, results suggested that enhanced ECM remodeling in the MRL forebrain allows for greater activity within the rostral migratory stream. Similarly, enhanced MMP expression in a variety of carcinomas has been noted to underlie increased tumor aggression and metastasis.[60-62] These studies are consistent with our findings of enhanced cellular migration and integration within the retina of the MRL mouse.

In conclusion, we have shown that MRL mice have the ability to modulate the MMP and ECM microenvironments within the retina. We further show that this alteration of the inhibitory molecular signals in the retina leads to decreased glial barrier formation at the level of the OLM that could allow incorporation of cells from grafted mature retinal tissue. Thus, we have identified conditions under which improved transplantation of mature retinal tissue may be possible.

Acknowledgements

Supported by National Eye Institute Grant 09595 (MJY), the Siegal Foundation, the Department of Defense, Natural Sciences and Engineering Research Council of Canada, the Lincy Foundation, and the Hoag Foundation.

References

1. Busch SA, Silver J. The role of extracellular matrix in CNS regeneration. Curr Opin Neurobiol 2007;17:120–127. [PubMed: 17223033]
2. Silver J, Miller JH. Regeneration beyond the glial scar. Nat Rev Neurosci 2004;5:146–156. [PubMed: 14735117]
3. Ponta H, Sherman L, Herrlich PA. CD44: from adhesion molecules to signalling regulators. Nat Rev Mol Cell Biol 2003;4:33–45. [PubMed: 12511867]

4. Moon LD, Asher RA, Fawcett JW. Limited growth of severed CNS axons after treatment of adult rat brain with hyaluronidase. J Neurosci Res 2003;71:23–37. [PubMed: 12478611]
5. Chaitin MH, Wortham HS, Brun-Zinkernagel AM. Immunocyto-chemical localization of CD44 in the mouse retina. Exp Eye Res 1994;58:359–365. [PubMed: 7513650]
6. Chaitin MH, Brun-Zinkernagel AM. Immunolocalization of CD44 in the dystrophic rat retina. Exp Eye Res 1998;67:283–292. [PubMed: 9778409]
7. Chaitin MH, Ankrum MT, Wortham HS. Distribution of CD44 in the retina during development and the rds degeneration. Brain Res Dev Brain Res 1996;94:92–98.
8. Inatani M, Tanihara H, Oohira A, Honjo M, Honda Y. Identification of a nervous tissue-specific chondroitin sulfate proteoglycan, neurocan, in developing rat retina. Invest Ophthalmol Vis Sci 1999;40:2350–2359. [PubMed: 10476802]
9. Zhang Y, Rauch U, Perez MT. Accumulation of neurocan, a brain chondroitin sulfate proteoglycan, in association with the retinal vasculature in RCS rats. Invest Ophthalmol Vis Sci 2003;44:1252–1261. [PubMed: 12601056]
10. Inatani M, Tanihara H, Oohira A, Honjo M, Kido N, Honda Y. Upregulated expression of neurocan, a nervous tissue specific proteoglycan, in transient retinal ischemia. Invest Ophthalmol Vis Sci 2000;41:2748–2754. [PubMed: 10937593]
11. Krishnamoorthy R, Agarwal N, Chaitin MH. Upregulation of CD44 expression in the retina during the rds degeneration. Brain Res Mol Brain Res 2000;77:125–130. [PubMed: 10814838]
12. Zhang Y, Klassen HJ, Tucker BA, Perez MT, Young MJ. CNS progenitor cells promote a permissive environment for neurite outgrowth via a matrix metalloproteinase-2-dependent mechanism. J Neurosci 2007;27:4499–4506. [PubMed: 17460063]
13. Yong VW, Power C, Forsyth P, Edwards DR. Metalloproteinases in biology and pathology of the nervous system. Nat Rev Neurosci 2001;2:502–511. [PubMed: 11433375]
14. Nagase H, Visse R, Murphy G. Structure and function of matrix metalloproteinases and TIMPs. Cardiovasc Res 2006;69:562–573. [PubMed: 16405877]
15. Ferguson TA, Muir D. MMP-2 and MMP-9 increase the neurite-promoting potential of Schwann cell basal laminae and are upregulated in degenerated nerve. Mol Cell Neurosci 2000;16:157–167. [PubMed: 10924258]
16. Turk BE, Huang LL, Piro ET, Cantley LC. Determination of protease cleavage site motifs using mixture-based oriented peptide libraries. Nat Biotechnol 2001;19:661–667. [PubMed: 11433279]
17. Kajita M, Itoh Y, Chiba T, et al. Membrane-type 1 matrix metalloproteinase cleaves CD44 and promotes cell migration. J Cell Biol 2001;153:893–904. [PubMed: 11381077]
18. Itoh Y, Seiki M. MT1-MMP: a potent modifier of pericellular microenvironment. J Cell Physiol 2006;206:1–8. [PubMed: 15920734]
19. Pizzi MA, Crowe MJ. Matrix metalloproteinases and proteoglycans in axonal regeneration. Exp Neurol 2007;204:496–511. [PubMed: 17254568]
20. Miyazaki K, Uchiyama K, Imokawa Y, Yoshizato K. Cloning and characterization of cDNAs for matrix metalloproteinases of regenerating newt limbs. Proc Natl Acad SciUSA 1996;93:6819–6824.
21. Vinarsky V, Atkinson DL, Stevenson TJ, Keating MT, Odelberg SJ. Normal newt limb regeneration requires matrix metalloproteinase function. Dev Biol 2005;279:86–98. [PubMed: 15708560]
22. Yang EV, Gardiner DM, Carlson MR, Nugas CA, Bryant SV. Expression of Mmp-9 and related matrix metalloproteinase genes during axolotl limb regeneration. Dev Dyn 1999;216:2–9. [PubMed: 10474160]
23. Park IS, Kim WS. Modulation of gelatinase activity correlates with the dedifferentiation profile of regenerating salamander limbs. Mol Cells 1999;9:119–126. [PubMed: 10340464]
24. Gross J. Getting to mammalian wound repair and amphibian limb regeneration: a mechanistic link in the early events. Wound Repair Regen 1996;4:190–202. [PubMed: 17177813]
25. Clark LD, Clark RK, Heber-Katz E. A new murine model for mammalian wound repair and regeneration. Clin Immunol Immunopathol 1998;88:35–45. [PubMed: 9683548]
26. Heber-Katz E. The regenerating mouse ear. Semin Cell Dev Biol 1999;10:415–419. [PubMed: 10497098]

27. Heber-Katz E, Chen P, Clark L, Zhang XM, Troutman S, Blanken-horn EP. Regeneration in MRL mice: further genetic loci controlling the ear hole closure trait using MRL and M. Wound Repair Regen 2004;12:384–392. [PubMed: 15225218]
28. Heber-Katz E, Leferovich J, Bedelbaeva K, Gourevitch D, Clark L. Conjecture: can continuous regeneration lead to immortality? studies in the MRL mouse. Rejuvenation Res 2006;9:3–9. [PubMed: 16608389]
29. Leferovich JM, Bedelbaeva K, Samulewicz S, et al. Heart regeneration in adult MRL mice. Proc Natl Acad Sci USA 2001;98:9830–9835. [PubMed: 11493713]
30. Leferovich JM, Heber-Katz E. The scarless heart. Semin Cell Dev Biol 2002;13:327–333. [PubMed: 12324214]
31. Mohand-Said S, Hicks D, Simonutti M, et al. Photoreceptor transplants increase host cone survival in the retinal degeneration (rd) mouse. Ophthalmic Res 1997;29:290–297. [PubMed: 9323720]
32. Silverman MS, Hughes SE. Transplantation of photoreceptors to light-damaged retina. Invest Ophthalmol Vis Sci 1989;30:1684–1690. [PubMed: 2527211]
33. Ogilvie JM, Speck JD, Lett JM, Fleming TT. A reliable method for organ culture of neonatal mouse retina with long-term survival. J Neurosci Methods 1999;87:57–65. [PubMed: 10065994]
34. Zhang Y, Caffe AR, Azadi S, van Veen T, Ehinger B, Perez MT. Neuronal integration in an abutting-retinas culture system. Invest Ophthalmol Vis Sci 2003;44:4936–4946. [PubMed: 14578420]
35. Yang L, Bula D, Arroyo JG, Chen DF. Preventing retinal detachment-associated photoreceptor cell loss in Bax-deficient mice. Invest Ophthalmol Vis Sci 2004;45:648–654. [PubMed: 14744910]
36. Young MJ, Ray J, Whiteley SJ, Klassen H, Gage FH. Neuronal differentiation and morphological integration of hippocampal progenitor cells transplanted to the retina of immature and mature dystrophic rats. Mol Cell Neurosci 2000;16:197–205. [PubMed: 10995547]
37. Inatani M, Tanihara H. Proteoglycans in retina. Prog Retin Eye Res 2002;21:429–447. [PubMed: 12207944]
38. Fisher SK, Lewis GP. Muller cell and neuronal remodeling in retinal detachment and reattachment and their potential consequences for visual recovery: a review and reconsideration of recent data. Vision Res 2003;43:887–897. [PubMed: 12668058]
39. Strongin AY, Collier I, Bannikov G, Marmer BL, Grant GA, Goldberg GI. Mechanism of cell surface activation of 72-kDa type IV collagenase: isolation of the activated form of the membrane metalloprotease. J Biol Chem 1995;270:5331–5338. [PubMed: 7890645]
40. Lim YT, Sugiura Y, Laug WE, Sun B, Garcia A, DeClerck YA. Independent regulation of matrix metalloproteinases and plasminogen activators in human fibrosarcoma cells. J Cell Physiol 1996;167:333–340. [PubMed: 8613475]
41. Siconolfi LB, Seeds NW. Mice lacking tissue plasminogen activator and urokinase plasminogen activator genes show attenuated matrix metalloproteases activity after sciatic nerve crush. J Neurosci Res 2003;74:430–434. [PubMed: 14598319]
42. Aramant R, Seiler M, Turner JE. Donor age influences on the success of retinal grafts to adult rat retina. Invest Ophthalmol Vis Sci 1988;29:498–503. [PubMed: 3343107]
43. Radtke ND, Aramant RB, Seiler MJ, Petry HM, Pidwell D. Vision change after sheet transplant of fetal retina with retinal pigment epithelium to a patient with retinitis pigmentosa. Arch Ophthalmol 2004;122:1159–1165. [PubMed: 15302656]
44. Aramant RB, Seiler MJ. Fiber and synaptic connections between embryonic retinal transplants and host retina. Exp Neurol 1995;133:244–255. [PubMed: 7649229]
45. Peng Q, Thomas BB, Aramant RB, Chen Z, Sadda SR, Seiler MJ. Structure and function of embryonic rat retinal sheet transplants. Curr Eye Res 2007;32:781–789. [PubMed: 17882711]
46. Thomas BB, Aramant RB, Sadda SR, Seiler MJ. Retinal transplantation: a treatment strategy for retinal degenerative diseases. Adv Exp Med Biol 2006;572:367–376. [PubMed: 17249598]
47. Thomas BB, Seiler MJ, Sadda SR, Aramant RB. Superior colliculus responses to light—preserved by transplantation in a slow degeneration rat model. Exp Eye Res 2004;79:29–39. [PubMed: 15183098]
48. Aramant RB, Seiler MJ. Progress in retinal sheet transplantation. Prog Retin Eye Res 2004;23:475–494. [PubMed: 15302347]

49. Radtke ND, Seiler MJ, Aramant RB, Petry HM, Pidwell DJ. Transplantation of intact sheets of fetal neural retina with its retinal pigment epithelium in retinitis pigmentosa patients. Am J Ophthalmol 2002;133:544–550. [PubMed: 11931789]
50. Wang X, Jung J, Asahi M, et al. Effects of matrix metalloproteinase-9 gene knock-out on morphological and motor outcomes after traumatic brain injury. J Neurosci 2000;20:7037–7042. [PubMed: 10995849]
51. Dubois B, Masure S, Hurtenbach U, et al. Resistance of young gelatinase B-deficient mice to experimental autoimmune encephalomyelitis and necrotizing tail lesions. J Clin Invest 1999;104:1507–1515. [PubMed: 10587514]
52. Gu Z, Cui J, Brown S, et al. A highly specific inhibitor of matrix metalloproteinase-9 rescues laminin from proteolysis and neurons from apoptosis in transient focal cerebral ischemia. J Neurosci 2005;25:6401–6408. [PubMed: 16000631]
53. Rosenberg GA, Navratil M, Barone F, Feuerstein G. Proteolytic cascade enzymes increase in focal cerebral ischemia in rat. J Cereb Blood Flow Metab 1996;16:360–366. [PubMed: 8621740]
54. Yang Y, Estrada EY, Thompson JF, Liu W, Rosenberg GA. Matrix metalloproteinase-mediated disruption of tight junction proteins in cerebral vessels is reversed by synthetic matrix metalloproteinase inhibitor in focal ischemia in rat. J Cereb Blood Flow Metab 2007;27:697–709. [PubMed: 16850029]
55. Romanic AM, White RF, Arleth AJ, Ohlstein EH, Barone FC. Matrix metalloproteinase expression increases after cerebral focal ischemia in rats: inhibition of matrix metalloproteinase-9 reduces infarct size. Stroke 1998;29:1020–1030. [PubMed: 9596253]
56. Chintala SK, Zhang X, Austin JS, Fini ME. Deficiency in matrix metalloproteinase gelatinase B (MMP-9) protects against retinal ganglion cell death after optic nerve ligation. J Biol Chem 2002;277:47461–47468. [PubMed: 12354772]
57. Heber-Katz E, Leferovich J, Bedelbaeva K, Gourevitch D, Clark L. The scarless heart and the MRL mouse. Philos Trans R Soc Lond B Biol Sci 2004;359:785–793. [PubMed: 15293806]
58. Hampton DW, Seitz A, Chen P, Heber-Katz E, Fawcett JW. Altered CNS response to injury in the MRL/MpJ mouse. Neuroscience 2004;127:821–832. [PubMed: 15312895]
59. Baker KL, Daniels SB, Lennington JB, et al. Neuroblast protuberances in the subventricular zone of the regenerative MRL/MpJ mouse. J Comp Neurol 2006;498:747–761. [PubMed: 16927265]
60. Bogaczewicz J, Jasielski P, Mosiewicz A, Trojanowski T, Suchozebrska-Jesionek D, Stryjecka-Zimmer M. [The role of matrix metalloproteinases and tissue inhibitors of metalloproteinases in invasion of tumours of neuroepithelial tissue]. Neurol Neurochir Pol 2006;40:404–412. [PubMed: 17103354]
61. Arvelo F, Cotte C. [Metalloproteinases in tumor progression: review]. Invest Clin 2006;47:185–205. [PubMed: 16886780]
62. Deryugina EI, Quigley JP. Matrix metalloproteinases and tumor metastasis. Cancer Metastasis Rev 2006;25:9–34. [PubMed: 16680569]

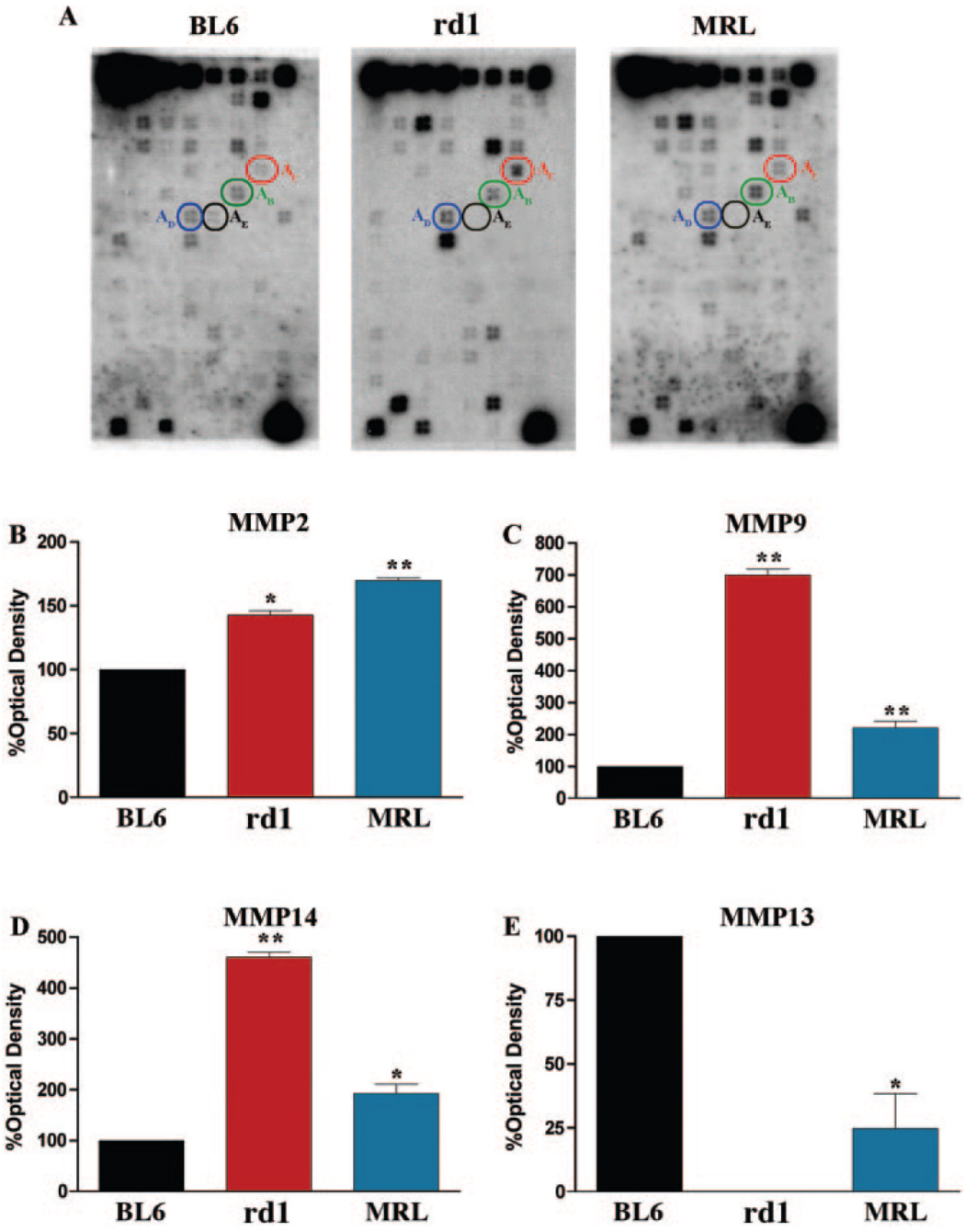

FIGURE 1.

ECM array gene expression analysis from BL6, rd1, and MRL mouse retinas. (**A-E**) Representative microarray gene chips for BL6 (**A1**), rd1 (**A2**), and MRL (**A3**) mice, with corresponding densitometric analysis of basal MMP-9 (**AB, B**), MMP-2 (**AC, C**), MMP-14 (**AD, D**), and MMP-13 (**AE, E**) RNA expression. Retinal expression of MMP-9 (**AB, B**), MMP-2 (**AC, C**), and MMP-14 (**AD, D**) RNA was significantly higher in rd1 and MRL mice than in BL6 wild-type controls. Retinal expression of MMP-13 (**AE, E**) was significantly lower in rd1 and MRL mice than in BL6 controls ($n = 12$). Significance was tested using one-way ANOVA, with Tukey testing for post hoc comparisons. *$P < 0.05$; **$P < 0.001$.

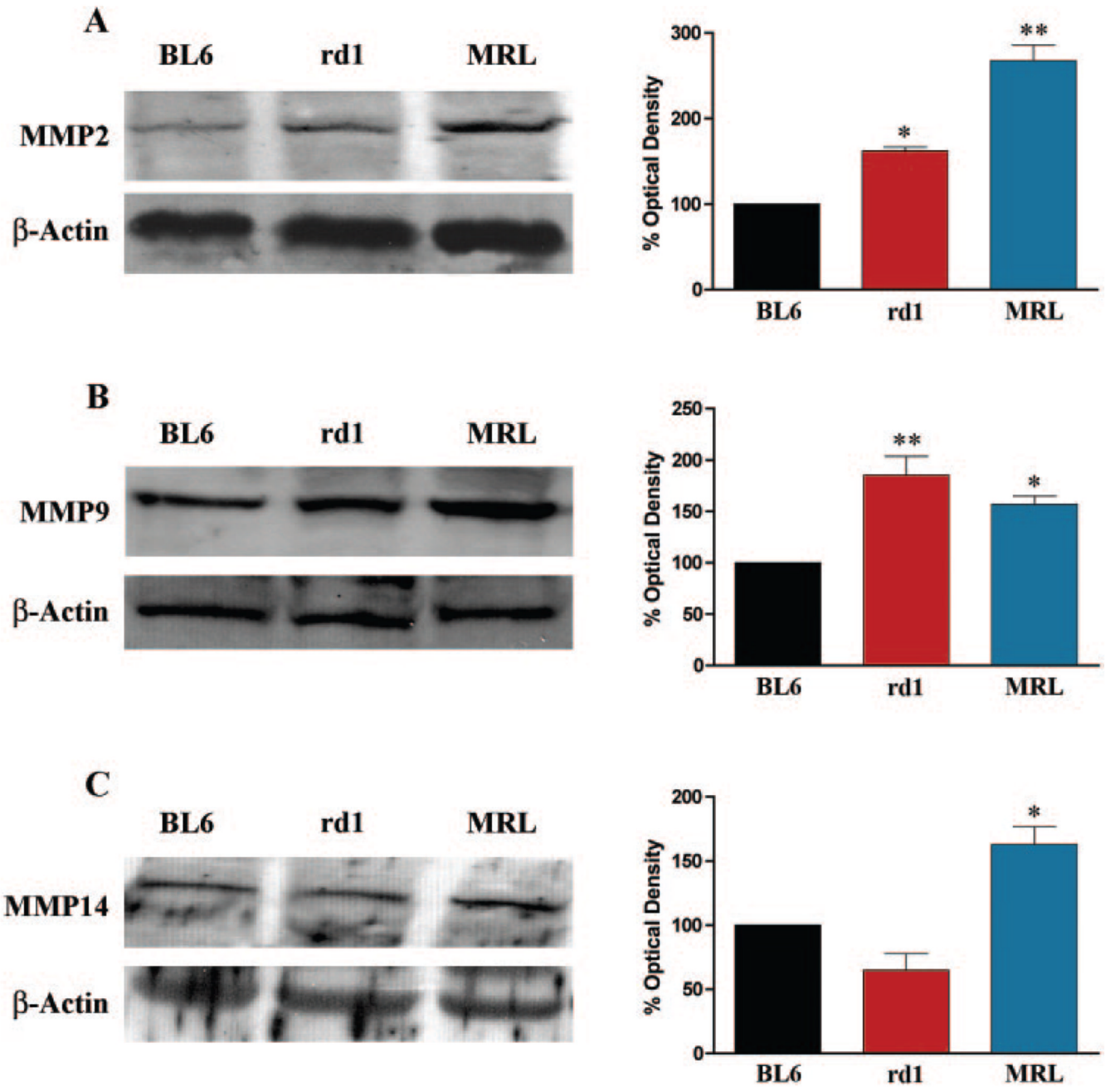

FIGURE 2.

Western blot analysis of MMP-2, -9, and -14 in adult BL6, rd1, and MRL mouse retina. (**A**-**C**) Representative Western blots and corresponding densitometric analyses of MMP-2 (**A**), MMP-9 (**B**), and MMP-14 (**C**) normalized against β-actin (loading control) in BL6, rd1, and MRL mouse retina explants. MMP-2 (**A**) and MMP-9 (**B**) expression was significantly higher in MRL and rd1 retinas than in BL6 wild-type controls. Similarly, a significantly higher level of MMP-14 (**C**) expression was detected in the MRL mouse retina than in the retina of rd1 injury and BL6 wild-type controls ($n = 12$). Significance was tested using one-way ANOVA with Tukey testing for post hoc comparisons. *$P < 0.05$; **$P < 0.001$.

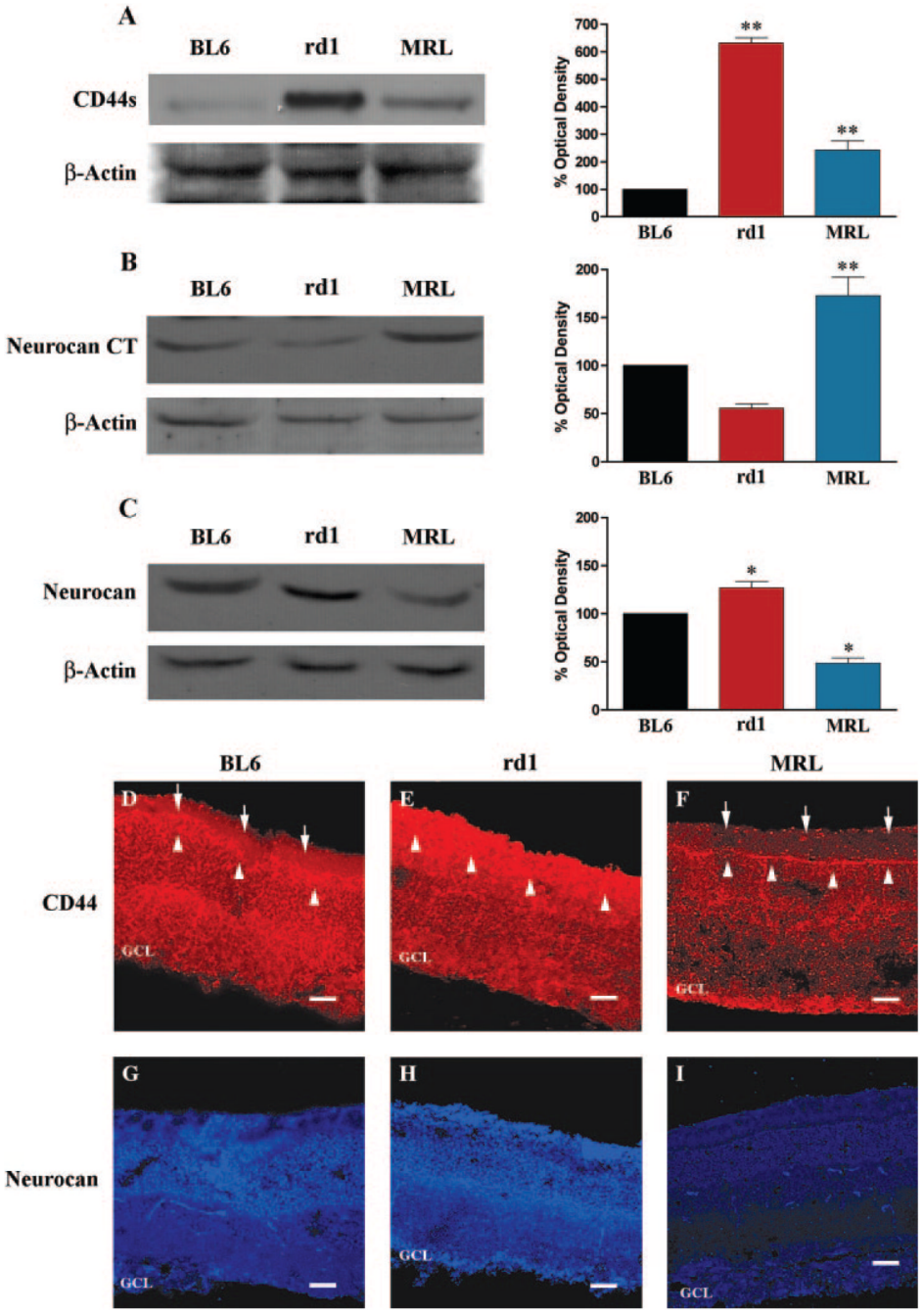

FIGURE 3.

Analysis of CD44 and neurocan expression in adult BL6, rd1, and MRL mouse retina explants. (**A**-**C**) Representative Western blots and corresponding densitometric analyses of CD44s (**A**, noninhibitory CD44 degradation product), neurocan (**B**), and neurocan-CT (**C**, noninhibitory c-terminal neurocan degradation product) normalized to β-actin (loading control) in BL6, rd1, and MRL mouse retina explants. CD44s (**A**) and neurocan-CT (**C**) expression was significantly higher, whereas full-length neurocan (**B**) expression was significantly lower in MRL mouse retina than in BL6 controls. CD44s (**A**) and full-length neurocan (**B**) expression were significantly higher in rd1 mouse retina than in B6 controls ($n = 12$). (**D**-**I**) Retinal explants were plated in serum-free media for 7 days and subsequently fixed, cryoprotected, sectioned,

and immunolabeled for full-length CD44 (**D**-**F**) and neurocan (**G**-**I**). Immunocytochemical staining revealed decreased CD44 (**F**) and neurocan (**I**) expression in MRL mouse retinas compared with B6 (**D**, **G**) and degenerative rd1 (**E**, **H**) controls ($n = 12$). Significance was tested using one-way ANOVA with Tukey testing for post hoc comparisons. *$P < 0.05$; **$P < 0.001$. Scale bar = 40 μm.

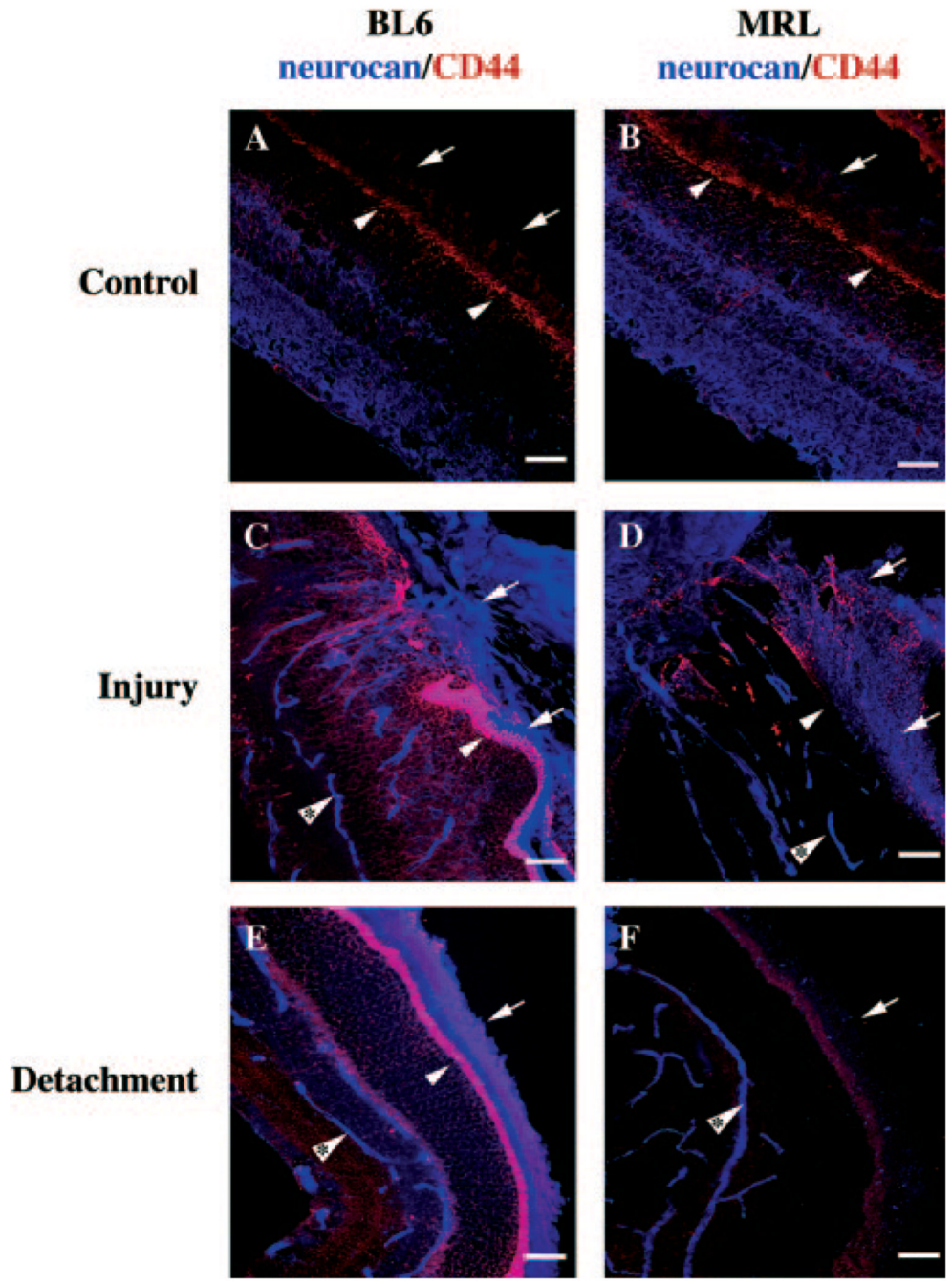

FIGURE 4.

Decreased CD44 and neurocan deposition in MRL mice after 14-day retinal detachment. Retinal detachments were induced by inserting a micropipette through the nasal retina and injecting 1 to 2 μL of 1.4% sodium hyaluronate into the subretinal space of age-matched BL6 and MRL mice. Eyes were enucleated 14 days after surgery and subsequently fixed, cryoprotected, sectioned, and immunostained. (**A**-**L**) Representative micrographs illustrating CD44 (*red*) and neurocan (*blue*) expression at injection and retinal detachment sites in BL6 (**A**, **C**, **E**) and MRL (**B**, **D**, **F**) mice ($n = 6$). Scale bar = 40 μm.

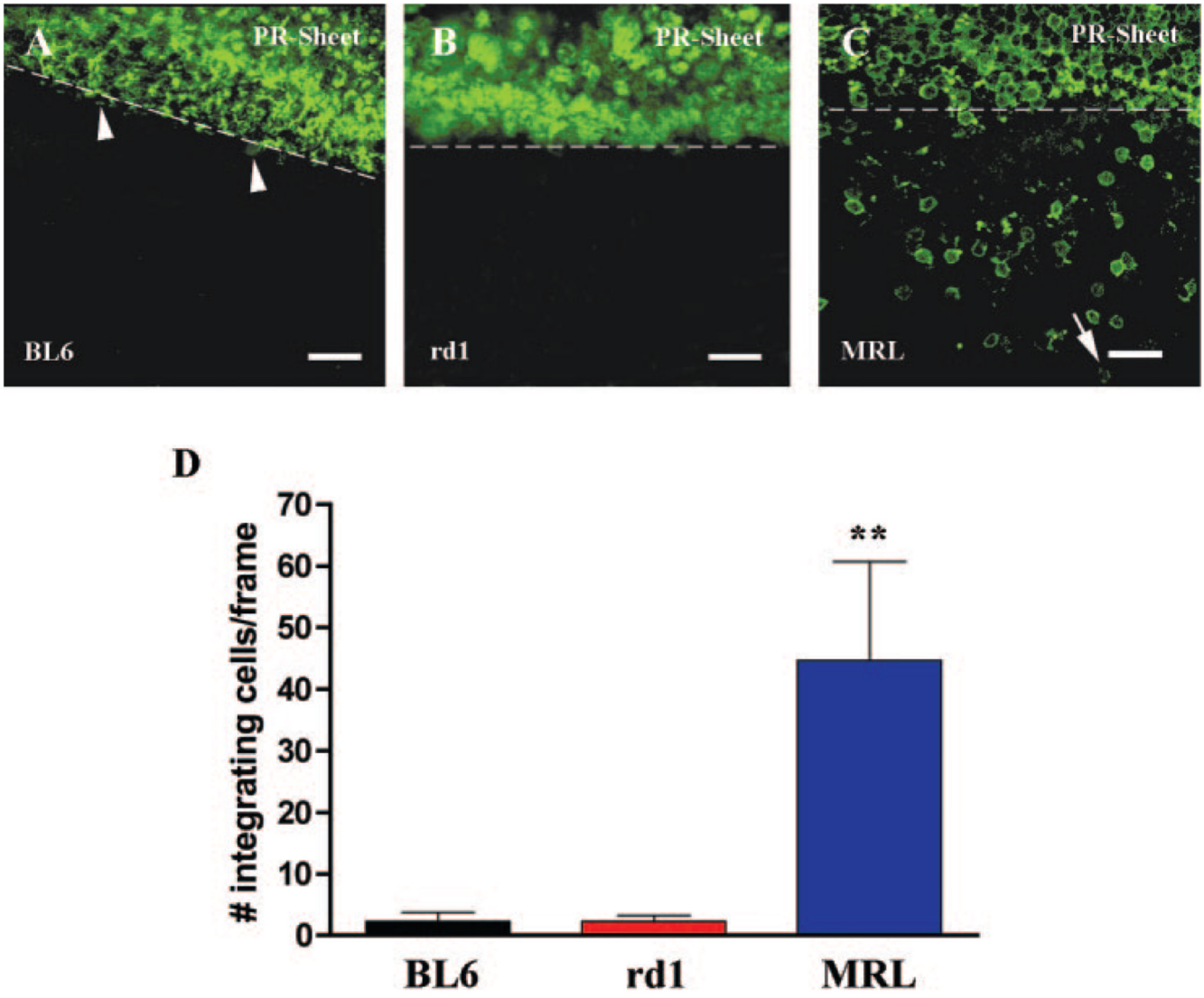

FIGURE 5.

Elevated MMP and subsequent decreased expression of CD44 and neurocan correlate with enhanced photoreceptor integration in the MRL mouse retina. Abutting retinal explants were performed in which GFP-positive photoreceptor sheets isolated from adult mice were transplanted on top of BL6, rd1, or MRL mouse retinas. Explants were cultured in serum-free neurobasal media for 7 days and subsequently fixed, cryoprotected, sectioned, and analyzed using confocal microscopy for GFP expression and subsequent cell counting. Although minimal photoreceptor integration was detected in abutting Bl6 (**A**, **D**) and rd1 (**B**, **D**) cultures, indicated by a lack of GFP-positive cells in the host tissue, increased integration of GFP-positive photoreceptor cells was detected in the MRL mouse retinas (**C**, **D**), indicated by numerous GFP-positive cells that have migrated to the host tissue ($n = 12$). Significance was tested using one-way ANOVA with Tukey testing for post hoc comparisons. $^{**}P < 0.001$. Scale bar = 20 μm.

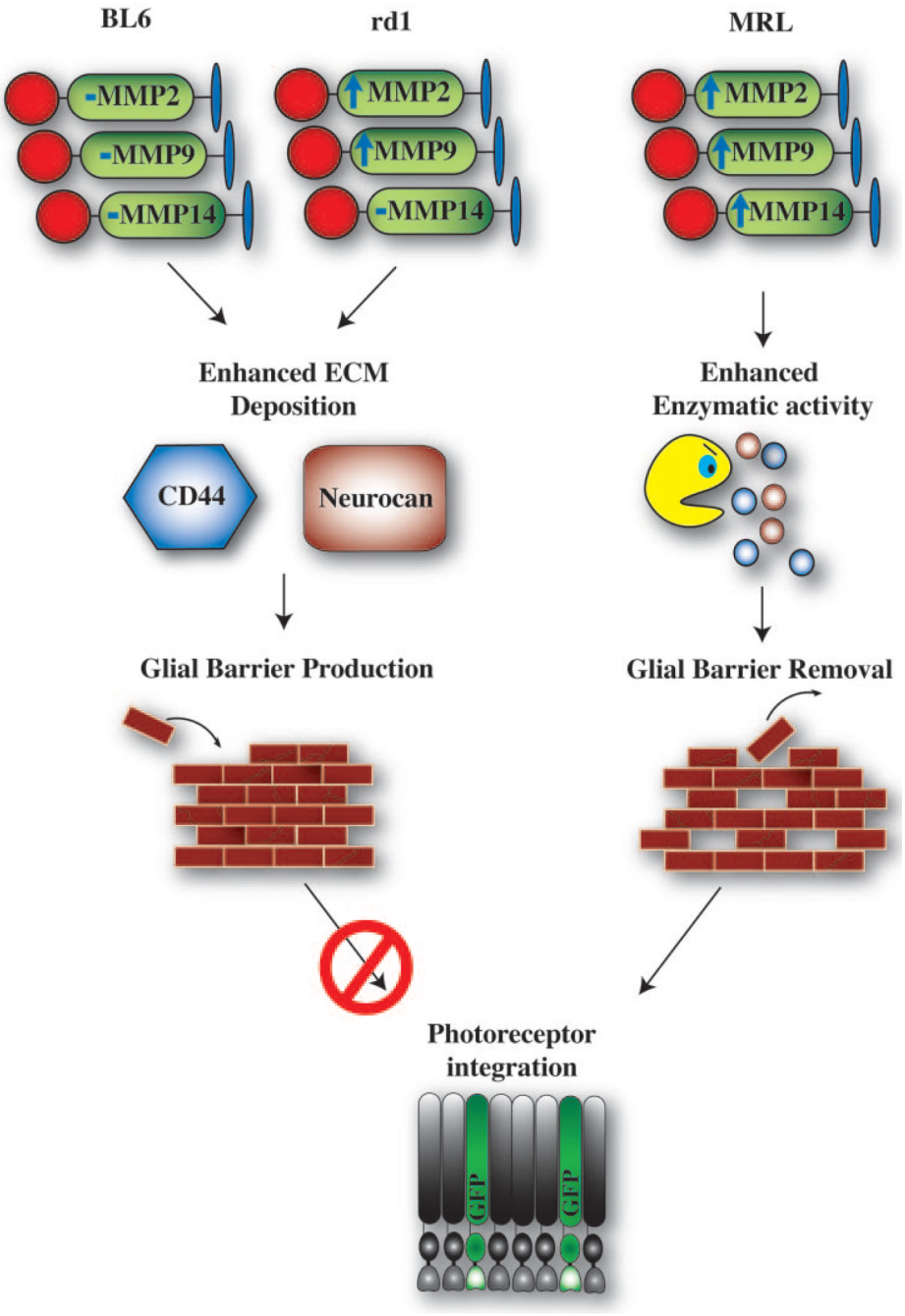

FIGURE 6.

Schematic diagram based predominantly on in vitro explant studies, summarizing the environmental differences among BL6, rd1, and MRL mouse retinas. Unlike the BL6, injury to the MRL mouse retina stimulated enhanced MMP-2, -9, and -14 expression, which led to enhanced enzymatic activity, glial barrier degradation, and photoreceptor integration. Although similar elevations in MMP-2 and -9 were observed in the rd1 mouse, inhibitory ECM deposition, poor glial barrier formation, and poor photoreceptor integration persisted.